Available online at www.sciencedirect.com

ScienceDirect

Procedia Manufacturing 34 (2019) 83–89

Procedia MANUFACTURING

www.elsevier.com/locate/procedia

47th SME North American Manufacturing Research Conference, Penn State Behrend Erie, Pennsylvania, 2019

Electroplastic effect on AA1050 plastic flow behavior in H24 tempered and fully annealed conditions.

Enrico Simonetto[a], Stefania Bruschi[a], Andrea Ghiotti[a,*]

[a]*University of Padua, Department of Industrial Engineering, Padova 35131, Italy*

* Corresponding author. Tel.: +39 049 8276822. *E-mail address:* andrea.ghiotti@unipd.it

Abstract

Electrically-Assisted (EA) technologies are emerging as a new category of forming processes, where the application of the electric field is used to assist the material deformation. The contribution of DC / AC electrical fields generally leads to a decrease of the flow stress and at the same time an increase of the material formability. However, the effects of the electrical current on the material behavior are still debated, since the thermal softening due to the concurrent temperature increase appears to be predominant for the larger ductility showed by the material. The present work aims at investigating the electro-plastic effect in AA1050 aluminum alloys sheets under two different states, namely the H24 tempered and the annealed conditions, by decoupling the electro-plastic and the thermal influence. Smooth specimens were tested along the three different rolling directions, applying different values of DC current in temperature-controlled conditions. For sake of comparison, the same tests were carried out by using an environmental chamber to reproduce the temperature increase due to the DC current.

Keywords: Sheet metal forming, Electroplasticity; Thermal effects; Aluminium alloy

1. Introduction

The last decades have seen an increased demand for new technologies capable of increasing the complexity of formed shapes for different material categories [1]. To meet these requirements new technologies were developed such as thermal assisted processes in order to increase the formability and to decrease the material flow stress [2]. However, other solutions have been explored, including the Electrically-Assisted (EA) processes that are emerging as a novel category. In these processes a Direct Current (DC) or pulsed/Alternate Current (AC) is applied to the part to achieve an increase in the material formability and a decrease in the material flow stress. In literature, several EA processes are proposed, such as rolling [3], blanking [4], sheet bending, [5] and microforming [6], but since the application of an electrical current is always coupled to a temperature increase due to the so-called Joule effect, it is not easy to distinguish the thermal effects from the electroplastic ones. At now in literature four different theories can be found to explain how the application of an electric current may contribute to the increase of the material formability: the most popular attributes to the presence of an electronic wind the increased annihilation of dislocations [7]. A second one explains the increased material ductility as a consequence of the dissolution of metallic bonds due to the increased electron presence in the crystal lattice [8]. A third one theorizes the presence of a microscale Joule heating in correspondence of the material discontinuities, such as the defects at the microscale [9]. Finally, the magneto-plasticity theory explains the reduction of the flow stress with the interaction between the dislocations and the magnetic field generated by the electric current [10]. In all these theories the

10.1016/j.promfg.2019.06.124

role of the dislocations seems to be of primary importance, and their interactions with the current flow determine the electroplastic behavior. Several authors studied the electroplastic effect under a wide range of conditions, testing different materials with different applied electric currents. The effect of pulsed DC or AC current were studied on aluminum alloys [11,12], steel [13] and magnesium alloys [14], but without the application of an effective cooling system to avoid the thermal effects. Other studies are focused on the effects of only DC current on titanium alloys [15], steels [16], copper and aluminum [17], but without a proper separation of the electroplastic and thermal effects. At the same time other researchers studied the electroplastic effect on materials with a different amount of initial cold working [18] or subjected to different thermal treatments [19,20], or the anisotropy effect on aluminum alloys combined with DC effects [21].

The aim of the present paper is to investigate the electroplastic effect when decoupled from the thermal softening, taking into account the influence of the initial work hardening and rolling direction. The alloy object of investigation is the AA1050, provided in two different conditions, namely H24 tempered and annealed (O). This allow comparing the influence of the electroplastic effect on the same material, with the same chemical composition and crystal lattice, but with two different initial amounts of work hardening and, therefore, different dislocation densities. Tensile tests along the three rolling directions with eight different levels of applied DC were performed. Thanks to a specifically designed cooling system, the material temperature was kept constant as much as possible during the test, in order to avoid the material softening and increased formability due to the joule heating. Furthermore, for sake of comparison, the same tensile tests were performed in an environmental chamber without the electrical current application, setting the test temperatures as close as possible to the ones measured during the EA tests.

2. Experiments

In this section, the reference material characteristics are presented together with the experimental equipment used to test the different conditions explained in the experimental plan.

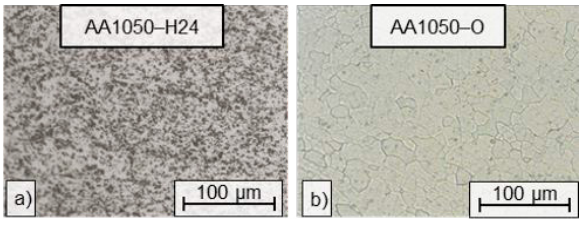

Fig. 1: Optical micrographs of the AA1050-H24 and AA1050-O in the as delivery conditions.

2.1. Material

The reference material was the AA1050, tested in two different states, namely the work hardened - partially tempered AA1050-H24 and the fully annealed AA1050-O. The AA1050 is known for its excellent corrosion resistance, high weldability and highly reflective finish and it is used for general purposes in different application fields such as furniture, heat exchangers or chemical plants. Both the materials were provided in sheets

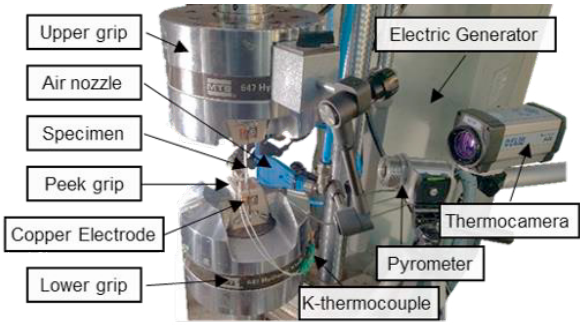

Fig. 2: Experimental equipment for the EA tensile tests.

(1000 x 2000 mm) with the thickness of 1.5(±0.1) mm. The microstructure of the material in the two states was observed using a Leica™ DMRE optical microscope. The samples were prepared for metallographic observations after cold mounting, grinding and polishing using the Keller's etchant to reveal the grain boundaries. Fig. 1 shows a comparison between the microstructure of the AA1050-H24 and AA1050-O in the as delivery conditions. When fully annealed, the material shows a more regular grain distribution than in the tempered conditions, since in this case the material was partially thermal treated after the mechanical deformation. The sheets have been cut by water jet in order to obtain the tensile specimens, whose geometry was defined according to the standards ISO6892 [22], having a gauge length of 65(±0.1) mm and a width of 12(±0.1) mm.

2.2. Experimental equipment

The tensile tests were carried out by using a 50 kN MTS™ dynamometer, equipped with special grips developed for EA tensile testing. Fig. 2 shows special grips made in polyether ether ketone (PEEK) with embedded copper electrodes. The PEEK grips ensure the insulation between the MTS frame and the specimens, in order to avoid current loses, while the embedded copper electrodes are connected to an industrial current generator. The current generator can provide a maximum power of 60 kW at a tension of 10 V and a current of 6000 A, with an accuracy of ±1 A. The experimental equipment includes two air nozzles, connected to a 10(±0.5) bar air compressor that blows the air on the specimen gauge length in order to keep the specimen temperature as closed as possible to the room one. The gauge length temperature was monitored during the tensile test by using the infrared thermo-camera FLIR™ A40. At the same time, a pyrometer was used to trigger the tensile test loading stage when the measured temperature reached an equilibrium condition. Both the systems were calibrated taking as reference the temperature measured by a k-type thermocouple spot-welded on the specimen. Furthermore, the deformation stage was recorded with a high-speed camera, in order to evaluate the specimen real strain by means of DIC techniques using the software GOM Aramis™. In the case of tests without the application of

the DC current, the dynamometer was equipped with an environmental chamber to perform hot test up to 350 °C and with an accuracy of ±2 °C.

2.3. Experimental plan

Table 1: Experimental plan for the EA tensile tests on AA1050.

DC density–A/mm²		0	5	10	15	20	25	30	35
Mat. state	Roll.dir.	Repeatability							
H24	0 deg	5	5	5	5	5	5	5	5
H24	45 deg	5	5	5	5	5	5	5	5
H24	90 deg	5	5	5	5	5	5	5	5
O	0 deg	5	5	5	5	5	5	5	5
O	45 deg	5	5	5	-	-	5	-	-
O	90 deg	5	5	5	-	-	5	-	-

The specimens were cut along the three different directions, with respect to the rolling one, namely 0 deg, 45 deg and 90 deg, for both the material states. Then eight different levels of DC density were applied for the different directions, all cooled by using the air nozzles. Tab. 1 shows the experimental plan for the EA tests. These values were selected according to the results reported in [23] in order to limit the joule heating. As show by Tab. 1, each condition was tested with a repeatability of 5, while along the 45 deg and 90 deg directions the annealed material was tested for the four different DC densities that were considered the most significant. By using an environmental chamber some thermal assisted tensile tests were carried out, on specimen cut along the rolling direction for three different temperatures consistent with the temperatures measured in the specimens during the EA tests. Tab. 2 shows the experimental plan for both the AA1050-O and AA1050-H24.

Table 2: Experimental plan for the thermal assisted tensile tests on AA1050.

Temperature - °C		25	50	75
Mat. State	Roll. dir.	Repeatability		
H24	0 deg	5	5	5
O	0 deg	5	5	5

3. Results

This section shows the comparison between the AA1050-H24 [23] and the AA1050-O behavior under the different testing conditions previously reported.

3.1. Thermo-electrical results

Fig. 3 shows the maximum temperature along the samples for different DC density values in the tested range, measured after reaching the equilibrium condition, just before the start of the tensile test loading stage. The maximum temperature with the cooling system is around 63 (±1.9) °C for a DC density of 35 A/mm² while without cooling the sample reach a maximum temperature over 400 °C for the same DC value. At the same time, for a DC density lower than 25 A/mm² the maximum temperature is lower than 45 °C with a difference from the baseline of 20 °C, so low enough to allow neglecting any thermal effect. The temperature distribution over the gauge length, for the minimum and maximum tested DC densities, shows a smooth thermal profile along the deformed length. The thermal distributions were analyzed for both the material states in the 3 rolling directions and did not show any difference for similar levels of the applied DC density.

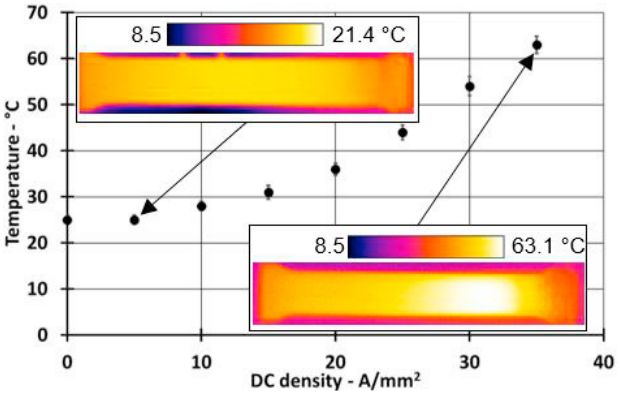

Fig. 3: Maximum sample temperature for different DC density in cooling conditions, and thermal profile along the specimen.

3.2. DC results

The mechanical results of the tensile test carried out on the AA1050-H24 are grouped in Fig. 4. In (a) the results carried out along the rolling directions are shown, for eight different DC densities, from 0 to 35 A/mm². The engineering strain – stress curves prove the low sensitivity of the UTS to the applied DC density. Having a high density of dislocations due to the pre-strained condition, the AA1050-H24 presents poor formability and low work-hardening exponent, which results in flat flow-stress curves with a final drop when the fragile rupture occurs. The material shows even a lower formability along the 45 deg (Fig. 4(b)) and 90 deg (Fig. 4(c)) if compared to the 0 deg direction. It can be seen that for a DC density of 5 A/mm² the strain at fracture has a maximum if compared with the baseline obtained without the application of any DC, especially at 0 deg and 90 deg. However, the relation between the applied DC densities and the material strain at fracture is not linearly monotonic, and, over 10 A/mm², the strain at fracture in lower than the baseline. The same trend is confirmed for all the three rolling directions, even if it is more relevant along the 0 deg and 90 deg than along the 45 deg directions. The same experimental plan, previously reported in Section 2.3, was carried out on the fully annealed AA1050-O.

Fig. 5 (a) shows the flow stress curves of the AA1050-O along the rolling direction. Since in the annealed condition the material has a lower dislocations density, the flow stress curves present a work hardening behavior and higher values of strain at fracture than the H24 condition, but, conversely, lower values of both the yield and Ultimate Tensile Strength (UTS). The results of the test carried out along the 45 deg (Fig. 5 (b))

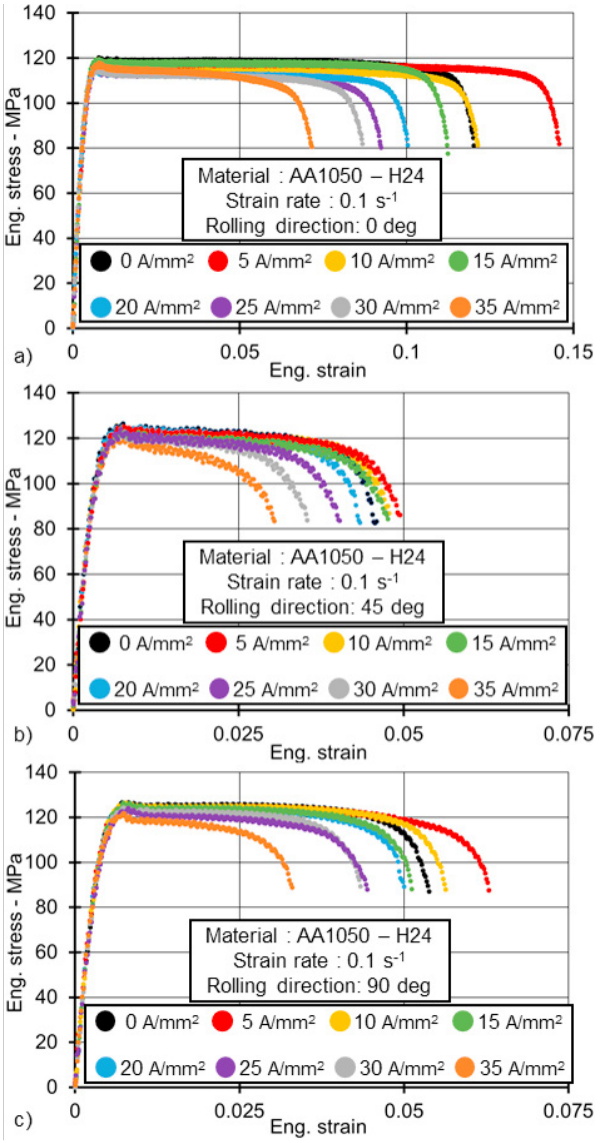

Fig. 4: Flow stress behaviour of the AA1050 – H24, for different DC density, with a strain rate of 0.1 s^{-1} along the tree rolling direction: a) 0dg, b) 45 deg and c) 90 deg.

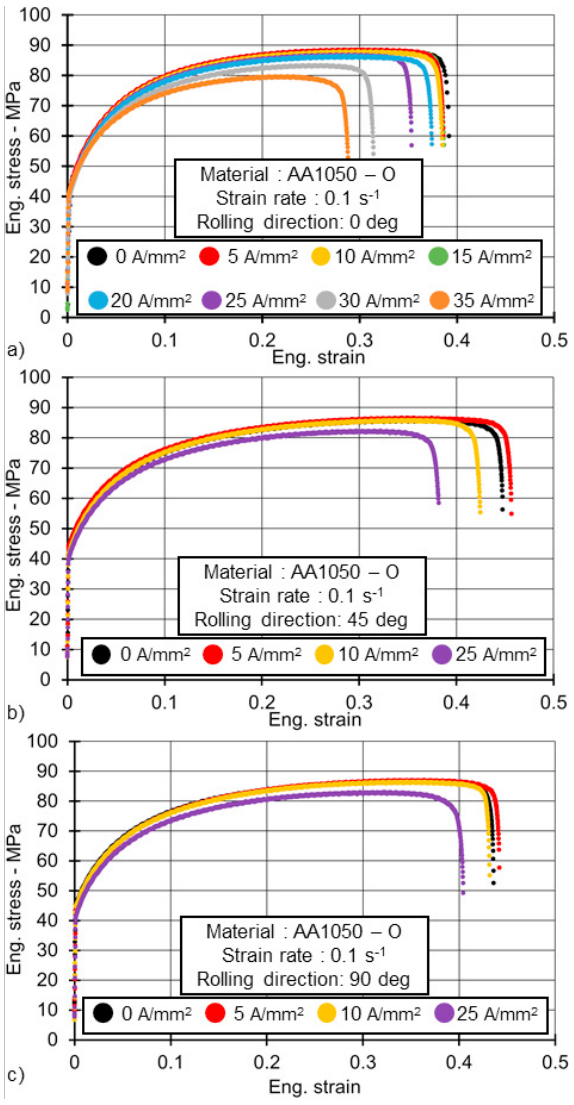

Fig. 5: Flow stress behaviour of the AA1050 – O, for different DC density, with a strain rate of 0.1 s^{-1} along the tree rolling direction: a) 0dg, b) 45 deg and c) 90 deg.

and 90 deg (Fig. 5(c)) directions show that the AA1050-O has a higher strain at fracture than in the 0 deg direction, for the same applied current density. Along the 0 deg direction, is was found that the higher the applied DC density the larger the decrease of both the flow stress and the strain at fracture. At the same time, the tensile tests carried out along the 45 deg and 90 deg directions showed that the DC density of 5 A/mm^2 maximize the strain at fracture.

3.3. Discussion – DC results

Having the two material conditions different flow stress behaviors, the effects of the applied DC density were compared on the basis of normalized values. The results were normalized with respect to the correspondent tests carried out without any applied current. Fig. 6(a) shows the comparison of the normalized values of the UTS obtained with the different DC densities, along the 0 deg direction for both the tempered and annealed conditions. It can be seen that the AA1050-H24 does not show any significant variation for DC densities lower than 25 A/mm^2, while the UTS value decreases for values higher than 30 A/mm^2 due to the Joule heating. In the same way, the AA1050-O shows a decrease of UTS values for DC density higher that 25 A/mm^2, and nearly no influence under this value. Fig. 6 (b) shows the same comparison on the UTS normalized values along the 45 deg and 90 deg directions. Even in this case, no relevant differences were detected neither for the annealed nor for the work-hardened condition.

Fig. 7 (a) shows the normalized strain at fracture along the 0 deg direction for both the AA1050-H24 and AA1050-O at different DC densities. The H24 condition has an increased

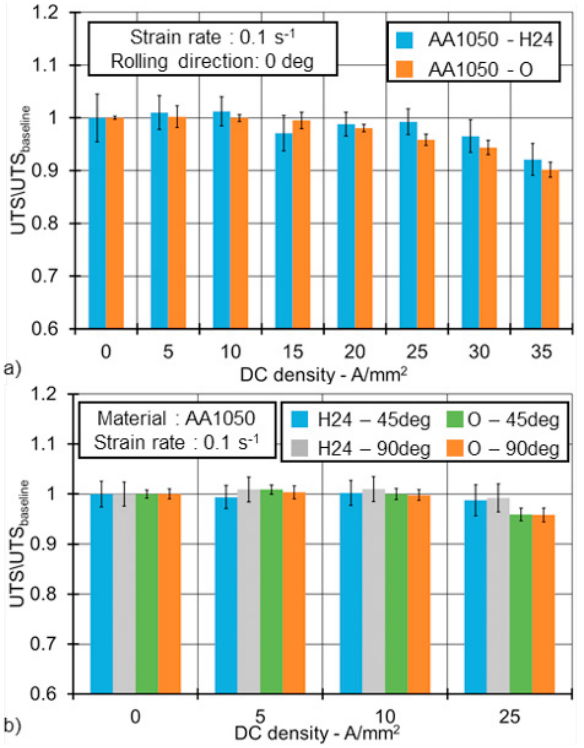

Fig. 6: Normalized UTS with different applied DC densities and materials state along the a) 0 deg direction, b) 45 deg and 90 deg directions.

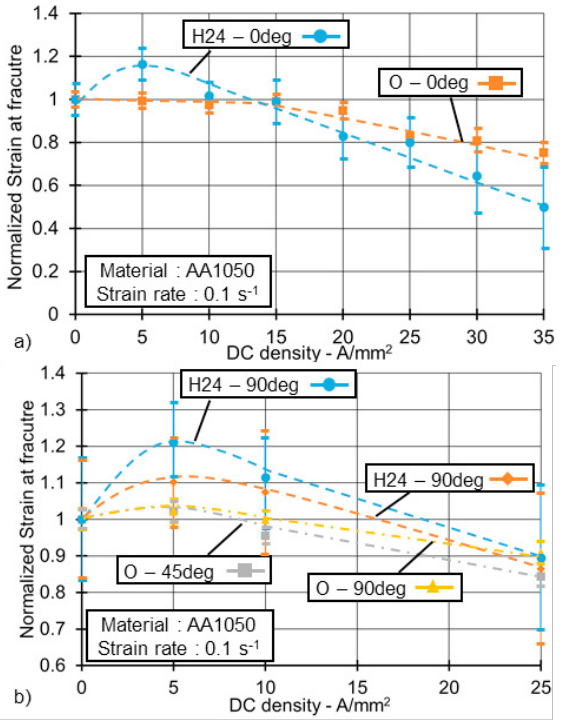

Fig. 7: Normalized strain at fracture with respect to the baseline vs DC density for the annealed and work hardened AA1050 along the: a) 0 deg, b) 45 deg and 90 deg rolling directions.

strain at fracture, with a maximum equal to 17% for the DC density of 5 A/mm^2; then the values decrease for higher values of current. Conversely, the annealed condition did not show any increase of the strain at fracture for any applied DC. The increased formability of the H24 at 5 A/mm^2 cannot be a consequence of the thermal effects since the temperature of the specimen was kept at room temperature, as it was measured during the tests by using both the pyrometers and the infrared thermos camera. So, the only contribution was given by the electro plastic effect that support the dislocations annihilation during the deformation. Such effect cannot be found in the annealed condition due to the fact that the initial dislocation density is significantly lower in this case. The same trend can be seen in Fig. 7 (b), for the 45 deg and 90 deg directions, with the AA1050-H24 that always shows an increase of the strain at fracture at 5 A/mm^2, equal to 20% and 9% respectively for the 90 deg and 45 deg specimens. Along these directions the annealed condition showed a slight increase in the strain at fracture, with a maximum increment of 2.2% at 5 A/mm^2.

3.4. Discussion – Thermal results

Both the material conditions were tested also in an environmental chamber at the same temperatures obtained in the DC current tests (see Fig. 3), namely 25 °C, 50 °C and 75 °C. The comparisons allow even more to distinguish the effects due to the thermal and electroplastic phenomena. Fig. 8 shows the normalized UTS with and without applied DC along the 0 deg direction. It can be noticed that the H24 condition shows higher values of UTS when a DC density is applied to the specimen compared to the tests carried out at the correspondent temperatures in the environmental chamber without the application of DC. At the same time, the annealed condition shows the opposite trend with a lower decrease of UTS obtained in tests carried out in the environmental chamber if compared with the tests at the correspondent temperatures under DC current application. In both cases, the higher the DC applied the higher the influence of the Joule heating, but in the H24 condition the application of a DC determine larger UTS values. Conversely, in the annealed condition the application of a DC determine lower UTS values, showing an opposite behaviour.

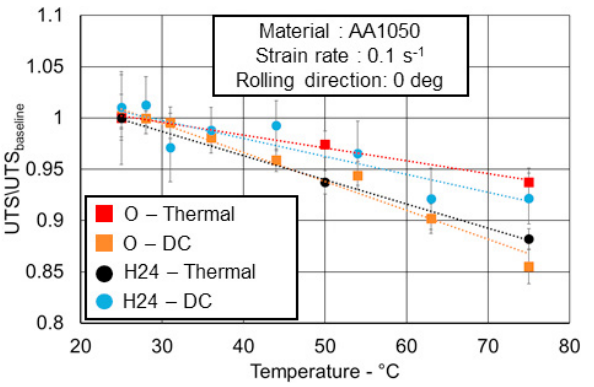

Fig. 8: Normalized UTS values at different testing temperatures obtained by means of an environmental chamber or by the effect of the DC current, with respect to the baseline condition for the two different material states

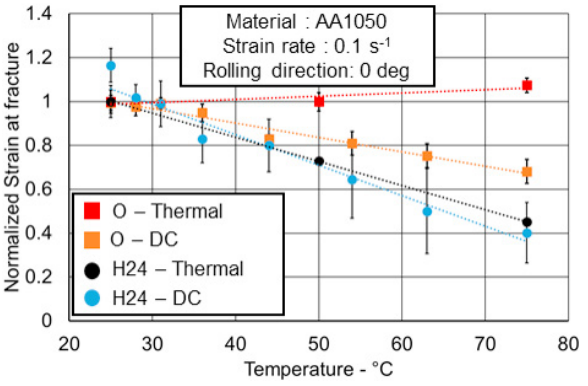

Fig. 9: Normalized strain at fracture at different testing temperature due to the Joule effect and obtained by means of an environmental chamber, with respect to the baseline condition for the two different material states

Fig. 9 shows the normalized strains at fracture with and without applied DC for both the tested material conditions. It was found that in the case of the annealed condition the specimens tested in the environmental chamber always reached higher strains at rupture than the specimens at the correspondent temperature under the application of a DC current. The same comparison for the H24 condition shows that the specimens tested with applied DC densities lower than 30 A/mm^2 have a higher strain at fracture than when tested in the environmental chamber. Higher levels of applied DC density lead to lower strain at fracture values compared with the results of the environmental chamber. It is worth noticing that this behaviour is opposite to the one of the annealed condition. Being the dislocation density the only difference between the two material states (due to a different amount of work hardening), this might confirm the interaction between the current flow and the dislocation density.

4. Conclusions

The paper presents the results of the investigations carried out on the AA1050 aluminum alloy, provided in H24 and annealed conditions, to assess the influence of the electro-plastic effect under the application of uni-axial deformations. The proposed methodology allowed decoupling the thermal effect due to the joule heating from the electro plastic one. The results show that the work-hardened condition is positively influenced by the electroplastic effect, with a peak of strain at rupture at 5 A/mm^2. This behavior was found for both the 0 deg and 90 deg directions, while a lower influence was seen along the 45 deg direction. On the other hand, the electroplastic effect did not cause any increase neither in terms of strain at fracture nor of UTS for the AA1050 in the annealed condition, independently from the tested directions. These opposite behaviors can be ascribed to the different amount of initial dislocation density in the two material states. The applied DC has a positive interaction with the condition having a higher density of dislocations, contributing to increase the strain at fracture. A set of tensile tests were carried out in an environmental chamber at temperatures consisted with the one reached during the EA tests. The comparison of the different conditions confirms the electroplastic effect leads to an increase of the mechanical properties of the AA1050-H24, while it decreases them in the case of AA1065-O.

References

[1] Tekkaya AE, Khalifa NB, Grzanicic G, Hölker R, Forming of lightweight metal components: Need for new technologies. Procedia Engineering, 2014, 81: 28 -37.

[2] Mori K, Bariani PF, Behrens BA, Brosius A, Bruschi S, Maeno T, Merklein M, Yanagimoto J, Hot stamping of ultra-high strenght steel parts. CIRP Annals – Manufacturing Technology, 2017;66:755–777.

[3] Zhu RF, Tang GY, Shi SQ, Fu MW, Effect of electroplastic rolling on the ductility ad superelasticity of TiNi shape memory alloy. Materials and Design, 2013;44:606-611.

[4] Kim M-J, Lee K, Hwan Oh K, Choi I.S, Yu H-H, Hong S-T, Han HN, Electric current-induced annealing during uniaxial tension of aluminum alloy. Scripta Materialia 2014;75:58–61.

[5] Egea AJS, Rojas HAG, Celentano DJ, Travieso-Rodrìgues JA, Fuentes JL, Electroplasticity-assiste bottom bending process. Journal of Materials Processing Technology, 2014;214:2261–2267.

[6] Jordan A, Kinsey BL, Investigation of thermal and mechanical effects during electrically-assisted microbending. Joruanl of Materials Processing technology, 2015;221:1-12.

[7] Conrad H, Spencher AF, Cao WD, Lu XP, Electroplasticiy- the effect of electricity on the mechanical properties of metals. The Journal of the Minerals Metals & Materials Society, 1990;42:38-33.

[8] Salandro WA, Jones J, Bunget C, Mears L, Roth J, Electrically assisted forming: modelling and control. Springer, Basel, Switzerland, 2015.

[9] Salandro WA, Bunget CJ, Mears L, Several factors affecting the electroplastic effect during an electrically-assisted forming process, Journal of Manufacturing Science and Engineering, 2011; 133-1-5.

[10] Molotskii MI, Theoretical basis for electro- and magnetoplasticity, Materials Science and Engineering, 2000; 287:248 – 258.

[11] Roh JH, Seo JJ, Hong ST, Kim MJ, Han HN, Roth JT, The mechanical behavior of 5052-H32 aluminum alloys under a pulsed electric current. International Journal of Plasticity, 2014; 58:84-99.

[12] Kim Mj, Lee MG, Hariharan K, Hong ST, Choi IK, Kim D, Oh KH, Han HN, Electric current – assisted deformation behavior of Al-Mg-Si alloy under uniaxial tension. International Journal of Plasticity, 2017; 94:148-170.

[13] Thien NT, Hong ST, Kim MJ, Han HN, Yang DH, Lee HW, Lee K, Electrically assisted dake hardening of complex phase ultra-high strenght steeels. Interantional Journal of Precision Engineering and Manufacturing, 2016; 17:225-231.

[14] Park JW, Jeong HJ, Jin SW, Kim MJ, Lee K, Kim JJ, Hong ST, Han HN, Effect of electric current on recrystallizaziont kinetics in interstitial free steel and AZ31 magnesium alloy. Material Characaterization, 2017; 133:70-76.

[15] Magargee J, Morestin F, Cao J, Characterization of flow stress for commercially pure titanium subjected to eletrically assisted deformation. Journal of Engineering Materials and Technology, 2013; 135:1-10.

[16] Kinsey B, Cullen G, Jordan A, Mates S, Investigation of elecroplasitc effect at high deformation rates for 403SS and Ti-6Al-4V. CIRP Annals – Manufacturing Technology, 2013, 62:279-282.

[17] Roh J-H, Seo J-J, Hong S-T, Kim M-J, Han HN, Roth JT, The mechanical behaviour of 5052-H32 aluminum under a pulsed electric current, International Journal of Plasticity, 2014;58:84-99.

[18] Siopis MS, Kinsey B, Experimental investigations of grain and specimen size effects during electrical-assisted forming, Journal of Manufacturing Science and Engineering, 2010: 132.

[19] Zheng YS, Tang GY, Kuang J, Zheng XP, Effect of electropulse on solid solution treatment of 6061 aluminum alloy, Jorunal of Alloys and Compounds, 2014;615:849-853.

[20] Pleta AD, Krugh MC, Nikhare C, Roth JT, An investigation on anisotropic behavior on 5083 aluminum alloy using electric current, ASME 2013 International Manufaturing Science and Engineering Conference Collocated with the 41st North American Manufaturing Research Conference, 2013.

[21] Breda M, Calliari I, Bruschi S, Forzan M, Ghiotti A, Michieletto F, Spezzapria M, Gennari C, Influence of stacking fault energy in electrically assisted uniaxial tension of FCC metals. Materials Science and Technology, 2016;33:317-325.
[22] ISO 6892-2:2018, International Organization for Standardization, Metallic materials – Tensile testing, 2018.
[23] Ghiotti A, Bruschi S, Simonetto E, Gennari C, Calliari I, Bariani PF, Electroplastic effect on AA1050 aluminium alloy formability. CIRP Annals – Manufacturing Technology, 2018;68:289-292.